



Joint time delay and frequency offset estimation scheme for multiple ONUs' activation in point-to-multipoint coherent PON system

YONGXIN XU,  XUDONG WANG,  WENQING JIANG, 
XIAOKAI GUAN,  MENGYUE SHI, WEISHENG HU, 
AND LILIN YI* 

State Key Lab of Photonics and Communications, School of Electronic Information and Electrical Engineering, Shanghai Jiao Tong University, Shanghai 200240, China

*lilinyi@sjtu.edu.cn

Abstract: For the next-generation access network standard, the coherent passive optical network (PON) using digital subcarrier multiplexing (DSCM) is a competitive candidate. The architecture employs time and frequency division multiple access (TFDMA) to improve network flexibility and access efficiency. Initial access to PON requires the activation of multiple optical network units (ONUs) to complete upstream synchronization. To meet the stringent latency requirements, the activation process of ONU should not cause significant delay and degradation for the transmission of upstream data. Therefore, we propose what we believe to be a novel ONU activation method for TFDMA coherent PON to jointly estimate time delay and frequency offset. The registration signal used for the ONU activation is designed as a combination of Zadoff-Chu sequence and Gold sequence, and the registration signal can be transmitted together with the data signal without the need for a quiet window. At the receiver, the time delay and frequency offset are estimated by calculating correlation values. Furthermore, successive interference cancellation is introduced to support simultaneous registration of multiple ONUs. The proposed activation scheme is validated in an coherent PON system with 6×10 GHz subcarriers. The experimental results show that the scheme can achieve a time delay estimation accuracy of 1 ns and frequency offset estimation accuracy of 1 MHz. Moreover, it does not cause any delay for upstream signal transmission, and the resulting SNR penalty is less than 0.2 dB.

© 2025 Optica Publishing Group under the terms of the [Optica Open Access Publishing Agreement](#)

1. Introduction

Driven by the sustainably growing traffic demand, the line rate of passive optical network (PON) is rising steadily. Considering the trends of previous standards proposed by both IEEE and ITU-T, 100 Gbps/200 Gbps and coherent detection will be the target peak rate and new architecture for the next generation PON [1–3]. Due to the digital subcarrier multiplexing (DSCM) technology, a single-wavelength coherent PON architecture using time and frequency division multiplexing (TFDM) becomes one of the most appealing options [4–7] for the next-generation PON. Different from coherent time-division-multiplexing (TDM)-PON and coherent wavelength-division-multiplexing (WDM)-PON, DSCM-based TFDM-PON can provide simple and flexible point-to-multipoint connections for different users without multiple wavelengths and optoelectronic components [8]. In addition to the requirements of higher capacity and flexibility, the incoming services such as 6 G fronthaul, industrial networks, business solutions and edge cloud require PON to have lower latency [9–11]. The latency requirements of certain services are even less than 100 us, which pose a significant challenge to PON system.

In the previous PON standards, the system architectures use intensity modulation and direct detection (IMDD), and the method of upstream transmission uses time division multiple access (TDMA). When an inactive optical network unit (ONU) first connects or reconnects to the PON,

optical line terminal (OLT) needs to perform discovery and ranging for the ONU by opening a quiet window to achieve upstream synchronization (i.e., the registration /activation process of ONU) [12]. During this process, OLT stops allocating upstream bandwidth to active (operational) ONUs, and then measures the arrival time of the upstream burst from the ONU to be registered. After ranging, the equalization delay is assigned to the ONU, so that it can participate in the upstream transmission without causing collisions with bursts from already active ONUs. When all ONUs complete registration, the transmission bursts from different ONUs are ordered.

However, the quiet window used in the registration process leads to inevitable pausing period. When the differential distance between OLT and ONU is 20 km, OLT needs to repeatedly pauses the upstream transmission with a quiet window of 250 μ s to allow the inactive ONU to implement the registration process [13]. It is challenging for ONUs to carry time-critical service. To solve this problem, many registration schemes are proposed to narrow or avoid quiet window. For example, the dedicated activation wavelength (DAW) scheme [14,15] introduced in 50G-PON standard allows ONU to be registered through a newly defined wavelength. The service wavelength is no longer allocated with quiet window, leading to a reduction in transmission delay. To reduce the inevitable pausing period and avoid the introduction of additional wavelength, multizone-based ONU activation scheme [16] is designed. According to the location of ONUs, different zones are flexibly configured. OLT sets different sizes of quiet windows for ONUs in different zones, so the pausing time caused by the quiet window can be effectively reduced. But this scheme fails to eliminate the quiet window. Delta-sigma modulation-based ONU activation scheme is proposed in [17], it takes the electrical tone signals of different frequencies with delta-sigma modulation as registration signal. The registration signal is directly superimposed on the regular upstream burst of the online ONU devices. This scheme ensures that the registration signal can be detected at very low power levels, thus eliminating the need for quiet window and not affecting the data signal.

Although these schemes can reduce the latency of the registration process, they are mostly focused on the typical IMDD PON with time division multiple access (TDMA). Some studies investigate single-wavelength PON using other multiple access technologies such as orthogonal frequency division multiple access (OFDMA) [18,19], but they only focus on the ranging problem, ignoring the issue of measuring the frequency offset of the transmitting laser. For DSCM-based coherent PON with TFDMA, different ONUs can utilize not only different time slot resources but also different subcarrier resources (subcarriers are not assigned to fixed ONUs). Therefore, the activation of ONU not only requires the time delay estimation (i.e. ranging), but also the estimation of frequency offset caused by uncalibrated laser. In this way, the signals of different ONUs do not collide in the time and frequency domains. Moreover, the activation scheme needs to be low-latency, compatible with coherent transceivers, and not interfere with data signals.

Therefore, we propose a novel ONU activation scheme for DSCM-based coherent PON with TFDMA. The registration sequence is designed as a combination of Zadoff-Chu sequence and Gold sequence, and then modulated into a narrow-bandwidth and low-speed signal located at the guard band. The registration signal is transmitted together with data signals, so the registration process does not require a quiet window. At the OLT, the time delay and frequency offset of the inactive ONU are estimated by calculating correlation values. Furthermore, to support simultaneous registration of multiple ONUs, successive interference cancellation mechanism is introduced. By recovering and eliminating the detected registration signals step by step, the receiver can improve its detection performance for the remaining registration signals. The proposed activation scheme is validated in the coherent PON system with 6×10 GHz subcarriers. The experimental results show that the scheme can achieve a time delay estimation accuracy of 1 ns and frequency offset estimation accuracy of 1 MHz. Moreover, it does not cause any delay for upstream signal transmission, and the resulting SNR penalty for data signal is less than 0.2 dB.

The remainder of the manuscript is organized as follows. Section 2 explains the principle of the proposed scheme. Section 3 depicts the experimental setup used to verify the performance of the proposed scheme. Section 4 presents and discusses the experimental results. We finally conclude in section 5.

2. Principle

The registration process of multiple ONUs can be regarded as a code division multiple access communication, where different ONUs to be registered can occupy the same time slot and frequency position, distinguished only by different registration codes. So the choice of registration code and the design of registration sequence are crucial. It requires that the self-correlation values of the sequences are large and the cross-correlation values between the sequences are small.

Common sequences include the Gold sequence, Zadoff-Chu (ZC) sequence and so on. The values in Gold sequence are +1 or -1. Figure 1 demonstrates the cross-correlation performance of the Gold sequence in the presence of time delay and frequency offset. Figure 1(a) illustrates a Gold sequence $G(n)$ with a length of 511, Fig. 1(b) depicts the cross-correlation of $G(n)$ and $G(n)$, Fig. 1(c) shows the cross-correlation of $G(n)$ and $G(n - d)$, where $G(n - d)$ is a time-delayed version of $G(n)$ with a delay of $d = 10$, Fig. 1(d) presents the cross-correlation of $G(n)$ and $G(n)e^{jwn}$, where $G(n)e^{jwn}$ is a frequency-offset version of $G(n)$ with a frequency offset of $w = 0.1$. By comparing Fig. 1(b)–(d), it is evident that the cross-correlation result lacks a distinct peak when a frequency offset is present. Consequently, the Gold sequence alone is unsuitable for registration scenarios involving frequency offsets.

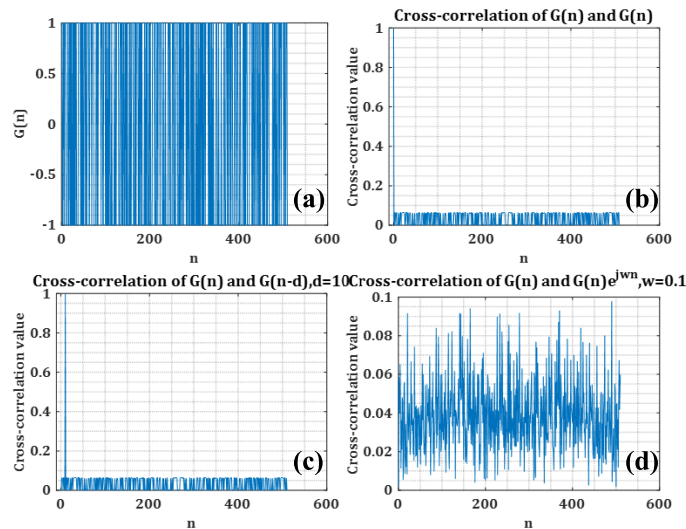


Fig. 1. (a) Gold sequence $G(n)$ with a length of 511. The cross-correlation results of (b) $G(n)$ and $G(n)$, (c) $G(n)$ and $G(n - d)$, where $d = 10$, (d) $G(n)$ and $G(n)e^{jwn}$, where $w = 0.1$.

Similarly, for ZC sequence, it can be expressed as (1), where ρ is its root value, L is the sequence length.

$$ZC(n) = \begin{cases} e^{-\frac{j\pi\rho n(n+1)}{L}} & L \text{ is odd} \\ e^{-\frac{j\pi\rho n^2}{L}} & L \text{ is even} \end{cases} \quad (1)$$

Figure 2 demonstrates the cross-correlation performance of the ZC sequence in the presence of time delay and frequency offset. The ZC sequence $ZC(n)$ with a length of 139 and $\rho = 13$

is shown in Fig. 2(a), and Fig. 2(b) depicts the cross-correlation of $ZC(n)$ and $ZC(n)$, Fig. 2(c) shows the cross-correlation of $ZC(n)$ and $ZC(n - d)$, where $ZC(n - d)$ is a time-delayed version of $ZC(n)$ with a delay of $d = 10$, Fig. 2(d) presents the cross-correlation of $ZC(n)$ and $ZC(n)e^{jwn}$, where $ZC(n)e^{jwn}$ is a frequency-offset version of $ZC(n)$ with a frequency offset of $w = 0.1$. By comparing Fig. 2(b)–(d), it can be found that the cross-correlation results of the ZC sequence exhibit distinct peaks in the presence of both time delay and frequency offset. This leads to ambiguity in the estimation of time delay and frequency offset. Consequently, the ZC sequence alone cannot meet the registration requirements either.

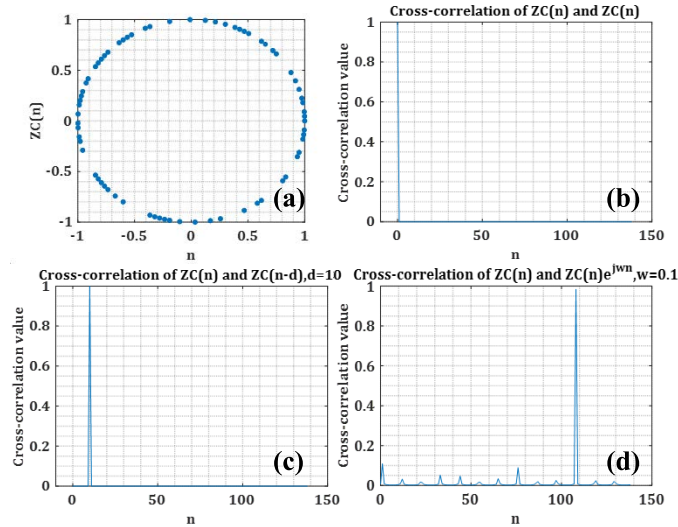


Fig. 2. (a) ZC sequence $ZC(n)$ with a length of 139. The cross-correlation results of (b) $ZC(n)$ and $ZC(n)$, (c) $ZC(n)$ and $ZC(n - d)$, where $d = 10$, (d) $ZC(n)$ and $ZC(n)e^{jwn}$, where $w = 0.1$.

Therefore, we use a combination of Gold sequence and ZC sequence as the registration sequence and employ spread spectrum communication technology to generate the registration signal. As shown in Fig. 3, registration sequence is designed as $[ZC\ ZC] \cdot * G_u$. It consists of two repeated ZC sequences of length L , each of which is upsampled s times (s is the spreading factor) and weighted by a Gold sequence $G_u(n)$ of length $N = 2sL$. ONUs to be registered randomly select Gold sequences from a predefined code set as $U = [1, 2, \dots, M]$, M is the size of code set, $u \in U$.

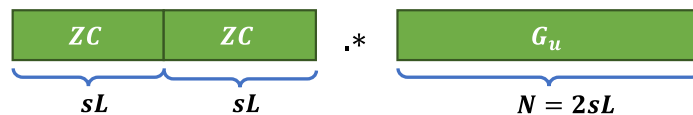


Fig. 3. Design of the registration sequence.

After ONU sends the registration signal, the OLT needs to process the received signal to determine whether the ONU is detected and to estimate its time delay and frequency offset.

Firstly, for the time delay estimation, the transmitted registration signal is denoted as $x(n)$, the received registration signal is denoted as $r(n)$, and the Gold sequence selected by ONU- i is

denoted as $G_u(n)$. Then, the timing metric function $M(d)$ can be calculated as (2),

$$M(d) = \frac{|P(d)|^2}{(R(d))^2} \quad (2)$$

$$P(d) = \sum_{m=0}^{sL-1} G_u(m)G_u(m+sL)r^*(d+m)r(d+m+sL) \quad (3)$$

$$R(d) = \frac{1}{2} \sum_{m=0}^{sL-1} r(d+m) \quad (4)$$

where $P(d)$ is the correlation of the received signal $r(n)$ and its delayed version with a delay of sL samples, $G_u(n)$ is applied to descramble the received signal $r(n)$, $R(d)$ is the instantaneous energy of $r(n)$ at the d -th sample used to normalize $P(d)$. The estimated time delay τ is given by (5),

$$\tau = \underset{d}{\operatorname{argmax}} M(d) \quad (5)$$

Secondly, for the frequency estimation, a blind frequency offset search (BFS) method is proposed. Specifically, the received registration signal $r(n)$ is compensated for time delay τ to obtain $r_{syn}(n)$. The frequency offset search step is set to Δf , and the range of search frequency offset f_b is from $-\frac{f_s}{2}$ to $\frac{f_s}{2}$, increasing by Δf each time. f_s is the sampling rate of signal. The frequency offset compensation and descrambling are performed for $r_{syn}(n)$ to obtain $r_{de}(n)$ as shown in (6),

$$r_{de}(n) = G_u(n)r_{syn}(n)e^{j2\pi f_b n/f_s} \quad (6)$$

then the peak value $C(f_b)$ of correlation between $r_{de}(n)$ and the transmitted ZC sequence is calculated as (7). Only with the correct frequency offset value, $C(f_b)$ can reach the maximum value, and the corresponding f_b is the estimated frequency offset f_{est} , which is given by (8).

$$C(f_b) = \left| \sum_{n=0}^{sL-1} r_{de}(n)ZC(n) \right| \quad (7)$$

$$f_{est} = \underset{f_b}{\operatorname{argmax}} C(f_b) \quad (8)$$

Thirdly, for the judgment of activation of registration sequence, the threshold detection approach is employed. According to (8), when $C(f_{est})$ exceeds the set detection threshold Th , the registration signal is considered to be successfully detected.

Finally, when multiple ONUs initiate registration in the same time slot and frequency position, the registration signals of other ONUs can cause interference to the registration signal of target ONU. Moreover, the detection performance will deteriorate as the number of ONUs increases. To solve this problem, a successive interference cancellation (SIC) mechanism is designed. At the receiver, the registration signals from different ONUs are superimposed. When one of the registration signals is successfully detected, we can identify the corresponding transmitted registration signal by the detected sequence code. Based on the transmitted and received signals, channel estimation can be performed to recover the received registration signal. Then, the recovered registration signal is removed from the total registration signals, thereby reducing interference and enhancing the success rate of detecting other registration signals. Finally, the SIC mechanism reconstructs and eliminates interference signals, completing the detection of all registration signals step by step. As shown in Fig. 4, the received registration signal vector $\mathbf{r} = [r(1), r(2), \dots, r(N)]^T$ first calculates the correlation values with the sequences $\{\mathbf{x}_u, u = 1, 2, \dots, M\}$ generated by the local registration code set U in the correlator according to (2) - (5). After compensating for the time delay, the frequency offset is estimated and compensated according to (6)–(8). When the detection result $C(f_b)$ does not exceed the set threshold Th , the detection process is stopped, otherwise the interference cancellation is started. At iteration k ,

assume $\{u_1, u_2, \dots, u_{k-1}\}$ are the detected registration codes, and the corresponding registration sequences generated from Fig. 3 are $\{x_{u_1}(n), x_{u_2}(n), \dots, x_{u_{k-1}}(n)\}$. During the SIC process, the channel estimation of the detected registration signal based on the least square error method [20, Chapter 6] is given by (9), the recovery of the detected registration signal is given by (10), and the interference cancellation is given by (11),

$$\mathbf{h}_{k-1} = (\mathbf{X}_{k-1}^H \mathbf{X}_{k-1})^{-1} \mathbf{X}_{k-1}^H \mathbf{r}_{k-1} \quad (9)$$

$$\mathbf{d}_{k-1} = \mathbf{X}_{k-1} \mathbf{h}_{k-1} \quad (10)$$

$$\mathbf{r}_k = \mathbf{r} - \sum_{i=1}^{k-1} \mathbf{d}_{k-1} \quad (11)$$

where $\mathbf{h}_{k-1} = [h_{k-1}(1), h_{k-1}(2), \dots, h_{k-1}(n_{taps})]^T$ is the estimated channel vector, n_{taps} is the channel length. $\mathbf{X}_{k-1} \in \mathbb{C}^{N \times n_{taps}}$ is the matrix generated by performing a sliding window on $x_{u_{k-1}}(n)$, $\mathbf{d}_{k-1} = [d_{k-1}(1), d_{k-1}(2), \dots, d_{k-1}(N)]^T$ is the recovered interference signal. $\sum_{i=1}^{k-1} \mathbf{d}_{k-1}$ are the accumulated recovered interference signals from the first $k-1$ iterations of detection. \mathbf{r}_k is the received signal vector at the k -th iteration that eliminates interference signals from the original received registration signal vector \mathbf{r} . Then SIC detection is continued for \mathbf{r}_k until the iteration is finished.

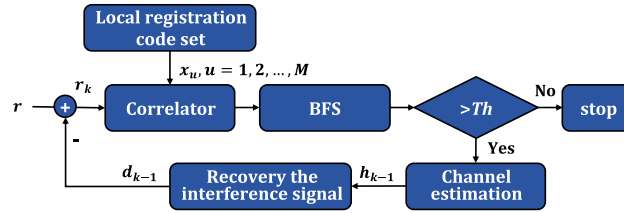


Fig. 4. Multiple registration signals detection framework based on successive interference cancellation.

3. Experimental setup

To investigate the feasibility of the proposed ONU activation scheme, we demonstrate a polarization-division multiplexed (PDM) coherent PON with 6×10 GHz subcarriers. The experimental setup is shown in Fig. 5(a), experimental system uses TFDM. Assume that the system has a total of P ONUs and they share 6 subcarrier resources as well as time-domain resources. The 6 subcarriers correspond to the data signals of ONU-1 to ONU-6, and the remaining ONUs need to initiate registration to access the system. The spectrum allocation of data signals and registration signals is shown in Fig. 5(b), the guard band between different subcarriers is set to 500 MHz, while the guard band at the center of frequency spectrum is 1.5 GHz, reserved exclusively for registration signals. In the experimental validation, since we have only one set of ONU equipment, the remaining subcarriers are simulated through digital subcarrier multiplexing. The registration signals with different parameters are transmitted with the sole ONU, and the parameters of the registration signal, such as relative power, time delay, and frequency offset, are set in the electrical domain. Figure 5(b) demonstrates the frequency spectrum of the received signal on X and Y polarization when the power of registration signal is 15 dB lower than that of the data signal.

The transmitter (Tx) and receiver (Rx) DSP procedures for data signal and registration signal are shown in Fig. 5(c) and (d), respectively. For data signal, random bits are firstly mapped to quadrature phase shift keying (QPSK) symbols. After the pulse shaping using a square root-raised cosine (RRC) filter with the roll-off factor of 0.1, the signal is resampled to match

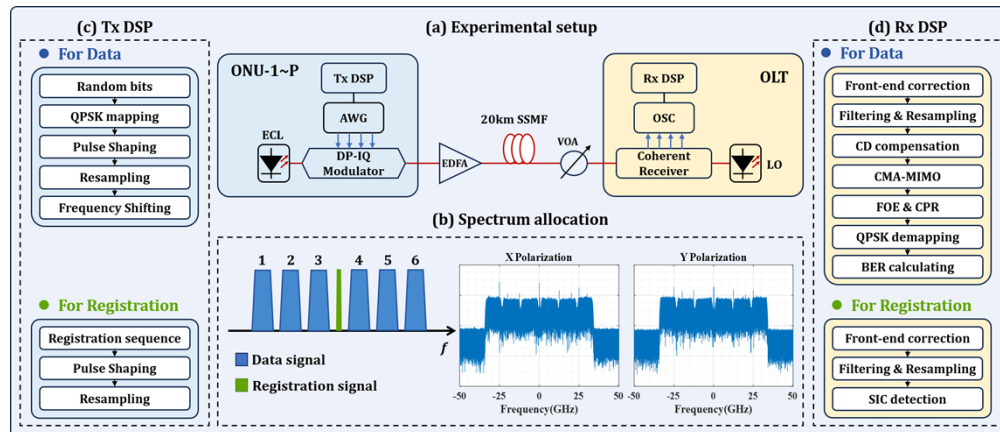


Fig. 5. (a) Experimental setup. (b) Spectrum allocation of data signals and registration signals, as well as the frequency spectrum of the received signal in X and Y polarization. DSP procedure for data signal and registration signal in (c) transmitter and (d) receiver.

the sampling rate of arbitrary waveform generator (AWG). Then the signal is shifted in the frequency domain, and converted to analog signal by the Fujitsu AWG operating at 80GSa/s. The electrical signal is modulated by a 40-GHz coherent driver modulator (CDM) to generate the optical signal. An external cavity laser (ECL) with linewidth of 100 kHz is used as the laser source at the transmitter. The wavelength of ECL is 1550 nm, and the output power is 10 dBm. An erbium-doped optical fiber amplifier (EDFA) is adopted to increase the launch power to 9.8 dBm, corresponding to a power of 2.02 dBm for each subcarrier. The optical signal is launched into the 20-km standard single-mode fiber (SSMF). At the receiver, a variable optical attenuator (VOA) is used to adjust the received optical power (ROP). Another ECL is used as the local oscillator (LO), of which the output power is 10 dBm. The optical signal is mixed with the LO in an integrated coherent receiver (ICR) for coherent detection. Then the detected signal is captured by a 100-GSa/s Tektronix digital storage oscilloscope (OSC) with a bandwidth of 33 GHz for off-line Rx DSP. Front-end correction is first performed on multiplexed subcarriers to compensate for in-phase and quadrature (IQ) skew and IQ imbalance. Then the subcarriers are demultiplexed through frequency shifting and low-pass filtering. After being resampled to 2 samples per symbol (sps), chromatic dispersion (CD) compensation, multi-input multi-output equalization based on constant modulus algorithm (CMA-MIMO), frequency offset estimation (FOE) and carrier phase recovery (CPR) are implemented on each subcarrier separately. Finally, QPSK demapping is performed, and bit error rate (BER) is calculated.

For registration signal, at the transmitter, in different time slots, ONU to be registered randomly selects a registration sequence to modulate, where the length L of ZC sequence is 127, spreading factor s is set to 2, the length N of registration sequence is 508, and the data rate of registration sequence is 500 MHz. A RRC filter with a roll-off factor of 0.1 is applied to the sequence to realize pulse shaping. Then the obtained registration signal is resampled to match the sampling rate of the AWG. The registration signal is transmitted on both polarizations. In TFDMA-PON, the registration signal is mixed with the data signals in the time domain, while in the frequency domain, the registration signal occupies a specific frequency position. At the receiver, after front-end correction and low-pass filtering, registration signal is separated from the mixed signals. Then the signal is resampled to 2 sps and SIC detection is performed on it. The detection is performed simultaneously on both polarizations, and the highest peak value of the cross-correlation result from the two polarizations is selected.

4. Results and discussion

We demonstrate the performance of the proposed activation scheme from three aspects: the detection effect of single ONU registration, the impact of registration signal on data signal, and the detection effect of multiple ONU registrations. The evaluation indicators for detection performance include time delay estimation accuracy and frequency offset estimation accuracy, as well as false alarm rate and missed detection rate [21]. False alarm rate is defined as the probability that an ONU does not initiate registration but is detected, while missed detection rate is defined as the probability that an ONU initiates registration but is not detected.

Firstly, for the detection of single ONU registration, we change the power of registration signal, and conduct 200 experiments under each power scenario. The ROP is set to -24 dBm, at which value the BER of a single ONU reaches a threshold of $1e-2$. In each experiment, the time delay and frequency offset of registration signal are set randomly, with the time delay ranging from 0 ns to 500 ns and the frequency offset ranging from -500 MHz to 500 MHz. At the receiver, we record the peak cross-correlation values between the registration signal and the correct sequence, as well as the peak cross-correlation values between the registration signal and other sequences. Then we perform histogram statistics on these values and observe that the peaks roughly followed a Gaussian distribution. Consequently, by fitting the peak results to a Gaussian distribution, two types of Gaussian distributions are obtained. The first type is the distribution of correlation peaks when the registration signal is correlated with the correct sequence, denoted as “right”. The second type is the distribution of correlation peaks when the registration signal is correlated with other sequences, denoted as “others”. According to the feature of Gaussian distribution, for two Gaussian distributions, $g_1(x) \sim N(u_1, \sigma_1^2)$, $g_2(x) \sim N(u_2, \sigma_2^2)$, assuming $u_1 > u_2$, the optimal detection threshold Th can be calculated as (12)

$$Th = \frac{(u_1\sigma_2^2 - u_2\sigma_1^2) - \sigma_1\sigma_2\sqrt{(u_1 - u_2)^2 - 2(\sigma_2^2 - \sigma_1^2)\ln\left(\frac{\sigma_1}{\sigma_2}\right)}}{\sigma_2^2 - \sigma_1^2} \quad (12)$$

When the power of registration signal is 15, 20, 25, and 30 dB lower than that of data signal, the distributions of detection results are shown in Fig. 6(a)–(d). The horizontal axis is the peak value v of correlation, and the vertical axis is the probability density function (PDF) f . $P_f = \int_{Th}^{+\infty} f(v)dv$, $P_m = \int_0^{Th} f(v)dv$, Th is the optimal detection threshold. From Fig. 6(a)–(d), it can be seen that as the power of registration signal becomes smaller, the mean value of the distribution represented by “right” decreases and its variance increases. Therefore, P_f and P_m gradually deteriorate. When the power of registration signal is 25 dB lower than that of data signal, $P_f = 3.44e-15$, and $P_m = 9.57e-15$, which remain at a very low level. It indicates that the proposed activation scheme can support a large dynamic power range.

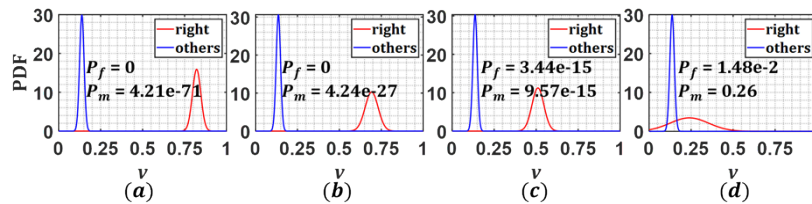


Fig. 6. The distributions of detection results when the power of registration signal is (a) 15, (b) 20, (c) 25 and (d) 30 dB lower than that of data signal.

The estimation errors of time delay and frequency offset during 200 experiments of single ONU registration are shown in Fig. 7(a)–(d). The top and bottom figures correspond to the time delay estimation error and frequency offset estimation error, respectively. The red cross “×” in the figures indicates that the registration signal is not successfully detected. From these figures, it can be seen that when the registration signal is correctly detected, the estimation errors of time delay and frequency offset are within ± 1 ns and ± 1 MHz, respectively.

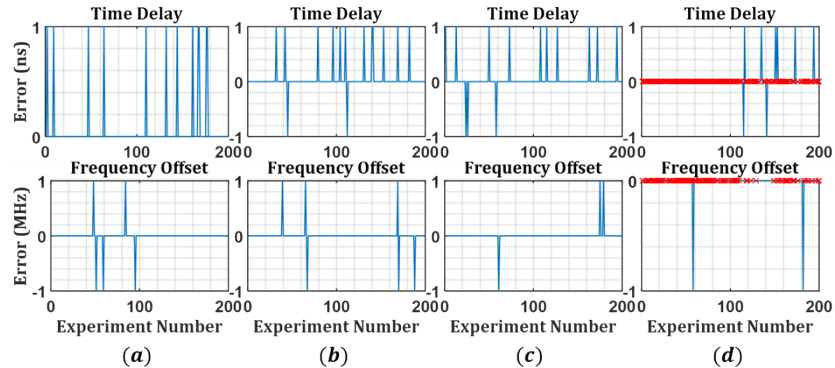


Fig. 7. The estimation errors of time delay (top) and frequency offset (bottom) when the power of registration signal is (a) 15, (b) 20, (c) 25 and (d) 30 dB lower than that of data signal.

Next, the impact of registration signal on data signal is evaluated. Since the laser of the ONU to be registered is not calibrated, there is spectrum overlap between the registration signal and the data signal, resulting in a degradation of signal-to-noise ratio (SNR). In the experiment, the power of registration signal is set to be 15 dB lower than that of data signal, the registration signal and the data signal on ONU-4 are set to have spectrum overlaps of 0%, 50% and 100%, respectively. Then, the BER variation of ONU-4 with ROP in different cases is counted to calculate the SNR penalty. The results are shown in Fig. 8, and it can be seen that according to the BER threshold of $1e-2$, the SNR penalty caused by the registration signal to the data signal is less than 0.2 dB, indicating that the registration process does not affect the normal communication of the data signal.

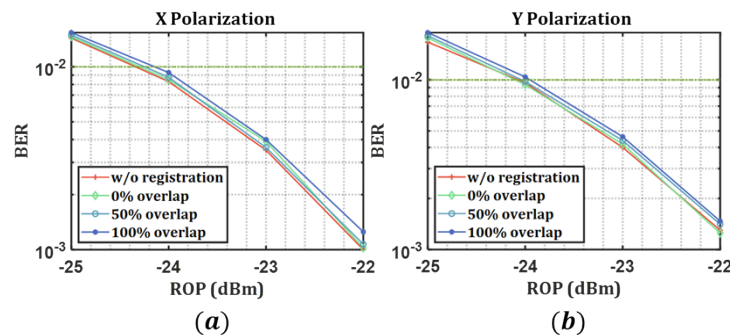


Fig. 8. The variation of BER with ROP for ONU-4 when there are different percentages of spectrum overlap between registration signal and data signal of ONU-4, where (a) is X polarization, and (b) is Y polarization.

Finally, the detection performance when multiple ONUs initiate registration is evaluated. We consider the worst-case registration situation, where all registration signals occupy exactly the

same time slot and spectrum position. When 3 ONUs initiate registration simultaneously, the distributions of detection results with and without SIC are shown in Fig. 9(a) and (b), respectively. In Fig. 9(b), “right- i ” represents the distribution of correlation peaks between the registration signal and the correct sequence during the i -th iterative detection process in SIC. Comparing the distributions of right-1 to right-3, it can be seen that the mean value of detection result keeps increasing as the interference is eliminated step by step. Figure 9(c) and (d) show the variation of false alarm rate and missed detection rate when different numbers of ONUs initiate registration simultaneously. It can be seen that P_f and P_m gradually deteriorate as the number of ONUs increases. Compared with the results without using SIC detection, the use of SIC can significantly reduce P_f and P_m , improve the detection effect and registration efficiency.

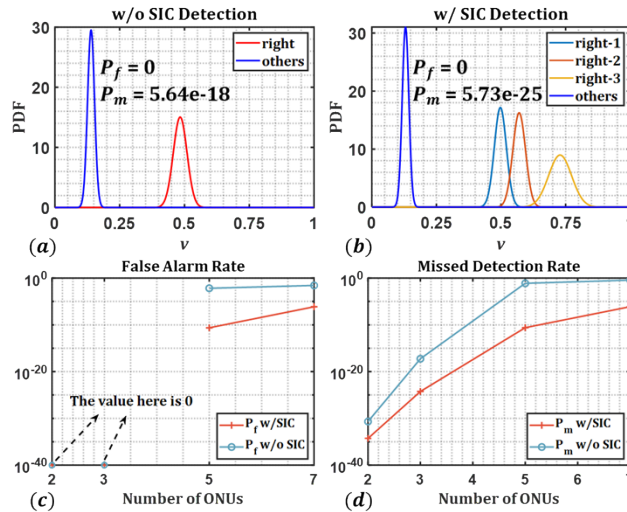


Fig. 9. The distributions of detection results for (a) not using SIC and (b) using SIC when 3 ONUs initiate registration simultaneously, and the comparison of (c) false alarm rate P_f and (d) missed detection rate P_m obtained with and without SIC for different numbers of ONUs.

SIC processes only one signal per iteration, enabling better interference elimination for each individual signal. However, this sequential processing necessitates that other signals await the completion of the detection process for the preceding ONUs, leading to significant detection delay when the number of ONUs is large. To address this limitation, parallel interference cancellation (PIC) can be considered as a viable alternative. In PIC, the receiver detects each ONU's signal at the same time in parallel, significantly reducing detection latency. Nevertheless, the simultaneous processing of multiple signals may compromise the effectiveness of interference cancellation, potentially leading to degraded detection performance. Consequently, accurate channel estimation and robust interference cancellation mechanisms become even more critical in PIC implementations. Furthermore, when the proposed registration method is extended to a larger scale of ONUs, the SNR of the registration signal will sharply decline due to the overlap between registration signals, and the SIC mechanism will reach its limit. In such cases, control and optimization strategies of medium access control (MAC) layer are required to provide assistance.

5. Conclusion

We propose and experimentally verify a novel ONU activation scheme for DSCM-based coherent PON system using TFDMA. By designing special registration sequence and signal, the registration process does not require the quiet window. Moreover, SIC-based correlation detection method is

designed to support multiple ONUs to initiate registration simultaneously. The experimental results show that the proposed scheme can realize a time delay estimation accuracy of 1 ns and a frequency offset estimation accuracy of 1 MHz. The scheme does not cause any delay for upstream signal transmission, and the resulting SNR penalty for data signal is less than 0.2 dB. In the future, we will further design a parallel interference cancellation detection scheme and optimize the complexity of the algorithm.

Funding. National Natural Science Foundation of China (62025503).

Disclosures. The authors declare no conflicts of interest.

Data availability. Data underlying the results presented in this paper are not publicly available at this time but may be obtained from the authors upon reasonable request.

References

1. M. S. Faruk, X. Li, D. Nessim, *et al.*, "Coherent Passive Optical Networks: Why, When, and How," *IEEE Commun. Mag.* **59**(12), 112–117 (2021).
2. J. Zhou, Z. Xing, H. Wang, *et al.*, "Flexible Coherent Optical Access: Architectures, Algorithms, and Demonstrations," *J. Lightwave Technol.* **42**(4), 1193–1202 (2024).
3. Z. Jia, H. Zhang, K. Choutagunta, *et al.*, "Coherent passive optical network: applications, technologies, and specification development [Invited Tutorial]," *J. Opt. Commun. Netw.* **17**(1), A71–A86 (2025).
4. Z. Xing, K. Zhang, X. Chen, *et al.*, "First Real-time Demonstration of 200 G TFDMA Coherent PON using Ultra-simple ONUs," in *Optical Fiber Communications Conference (OFC)*, (2023), paper Th4C.4.
5. J. Li, R. Fan, Q. He, *et al.*, "Bidirectional TFDMA 200 G coherent PON with a simplified receiver at the ONU side," *Opt. Lett.* **49**(18), 5127–5130 (2024).
6. M. Xu, Z. Jia, H. Zhang, *et al.*, "Intelligent burst receiving control in 100 G coherent PON with 4× 25 G TFDMA upstream transmission," in *Optical Fiber Communications Conference (OFC)*, (2022), paper Th3E.2.
7. H. Zhang and Z. Jia, "100 G TFDMA Coherent PON Featuring Burst Signal Processing in Digital Subcarriers," *ICC 2023 - IEEE International Conference on Communications*, 3302–3307 (2023).
8. D. Welch, A. Napoli, J. Back, *et al.*, "Point-to-Multipoint Optical Networks Using Coherent Digital Subcarriers," *J. Lightwave Technol.* **39**(16), 5232–5247 (2021).
9. X. Liu, "Enabling Optical Network Technologies for 5 G and Beyond," *J. Lightwave Technol.* **40**(2), 358–367 (2022).
10. A. Fayad, T. Cinkler, and J. Rak, "Toward 6 G Optical Fronthaul: A Survey on Enabling Technologies and Research Perspectives," *IEEE Commun. Surv. Tutor.* **27**(1), 629–666 (2025).
11. B. Cao, Q. Zhao, Y. Hong, *et al.*, "Network performance evaluation criterion model based on large connections for low latency in industrial 50G-PON network," *Opt. Fiber Technol.* **90**, 104107 (2025).
12. T. Horvath, P. Munster, V. Oujezsky, *et al.*, "Activation Process of ONU in EPON/GPON/XG-PON/NG-PON2 Networks," *Appl. Sci.* **8**(10), 1934 (2018).
13. T. Pfeiffer, P. Dom, S. Bidkar, *et al.*, "PON going beyond FTTH [Invited Tutorial]," *J. Opt. Commun. Netw.* **14**(1), A31–A40 (2022).
14. J. S. Wey, Y. Luo, T. Pfeiffer, *et al.*, "5 G Wireless Transport in a PON Context: An Overview," *IEEE Commun. Stand. Mag.* **4**(1), 50–56 (2020).
15. ITU-T, "Higher speed passive optical networks - common transmission convergence layer specification," ITU-T G.9804.2, (2021).
16. K. Kim, K. Doo, H. S. Chung, *et al.*, "Demonstration of Low Latency 25 G TDM-PON with Flexible Multizone-based ONU Activation for Time Critical Services," in *European Conference on Optical Communication (ECOC)*, (2022), paper Tu5.47.
17. Y. Zou, B. Li, L. Zhong, *et al.*, "DSM-Based Ultra-Low-Latency ONU Activation for Uninterrupted TDM-PON Services," *J. Lightwave Technol.* **42**(1), 128–135 (2024).
18. A. Razmtouz, K. Habel, C. Kottke, *et al.*, "Initial ranging scheme based on interpolated Zadoff-Chu sequences for OFDMA-PON," *Opt. Express* **22**(3), 3669–3674 (2014).
19. A. G. Reza, G. Y. Kim, M. S. Lee, *et al.*, "Zadoff-Chu sequence-based upstream ranging in OFDMA-PON mobile radio access networks," *Opt. Express* **26**(13), 17662–17668 (2018).
20. Y. S. Cho, J. Kim, W. Y. Yang, *et al.*, "MIMO-OFDM wireless communications with MATLAB," John Wiley & Sons, (2010).
21. Y. Wu, X. Gao, S. Zhou, *et al.*, "Massive Access for Future Wireless Communication Systems," *IEEE Wirel. Commun.* **27**(4), 148–156 (2020).